Strange Hadron Production for Au-Au Collisions

PHYS 267, Data Analysis Final Project

Brandon Huh, Yun Lee, and Francis Gerard Mozo

Department of Physics and Astronomy
University of Waterloo
August 11, 2023

Final Project: Strange Hadron Production for Au-Au Collisions

Brandon Huh, Yun Lee, and Francis Gerard Mozo

Abstract

We analyze the average transverse mass and antibaryon-to-baryon ratios for the strange hadron Λ in Au+Au collisions for various centre-of-mass energies, ranging from 7.7-39 GeV. First, we model and fit the transverse mass and antibaryon-to-baryon ratios using polynomial functions to determine the best model-fitted plot for each variable. Next, we conduct hypothesis testing using a two-sample unpaired t-test to determine whether the data sets are significantly different for the antibaryon-to-baryon ratio data. The result yields a p-value less than 0.05, rejecting the null hypothesis and concluding that the data sets of 19.6 GeV and 27 GeV are significantly different. A one-way ANOVA test was used for the transverse mass data to determine whether there are significant changes in the transverse mass within the centre-of-mass energy from 7.7-39 GeV. The p-value for this test was less than 0.05, thus rejecting the null hypothesis and concluding that there are significant differences in the transverse mass within the five different center-of-mass energies.

1. Introduction

Scientists make neutrino beams by colliding protons into nuclear targets in accelerator-based neutrino experiments. When this occurs, secondary hadrons are produced and these hadrons eventually decay to help produce the overall neutrino flux. Thus, measuring the production of these hadrons accurately is important in the production of neutrino flux. In the experiment by Adam et al. 2020, scientists studied the production of strange hadrons in collisions of gold nuclei at high speeds. They used this data to find information about the momentum and mass of the hadrons. In this data analysis report, we use the STAR measurements from Adam et al. 2020 to determine whether there are any significant changes in one set of data from 7.7-39 GeV for $\sqrt{s_{NN}}$, which is the centre-of-mass energies. The measurements we used are the averaged transverse mass and the antibaryon-to-baryon ratios as functions of the average number of participant nucleons, $\langle N_{part} \rangle$ for the strange hadron Λ. The hypothesis of this data analysis is that the data sets of different energy levels are significantly different for the average transverse mass and antibaryon-to-baryon ratios. The variables in this experiment include the average number of participant nucleons, $\langle N_{part} \rangle$, which is the independent variable. The dependent variables include the transverse mass and antibaryon-to-baryon ratios. Antibaryon-to-baryon ratios in Adam et al. 2020 are used to test model predictions in central collisions for all energies. In this report, we display the STAR measurement data of the transverse mass and antibaryon-to-baryon ratios using bar, pie, and line charts. In Section 3.1, we conduct our first analysis by modelling and fitting the antibaryon-to-baryon ratio and transverse mass data and present the plotted models for all energy levels. Section 3.3 and Section 3.4 covers our analysis using a two-sample independent t-test and one-way ANOVA test to test our hypothesis that there are significant differences between the energy level data sets.

2. Results

Using Python, the data was plotted using a variety of graphing methods. The first method, shown in Figure 1 and Figure 2, displays two side-by-side bar charts of the transverse mass and antibaryon-to-baryon ratios as a function of $\langle N_{part} \rangle$, respectively. The bars overlap in these charts because of varied $\langle N_{part} \rangle$ values for each energy level. Two additional charts in Figure 3 and Figure 4 display the total transverse mass and antibaryon-to-baryon ratios for each energy level from 7.7-39 GeV in the form of pie charts. The last two charts in Figure 5 and Figure 6 utilize line charts, where they plot the antibaryon-to-baryon ratio and transverse mass as a function of $\langle N_{part} \rangle$, respectively.

The most suitable presentation for this type of data

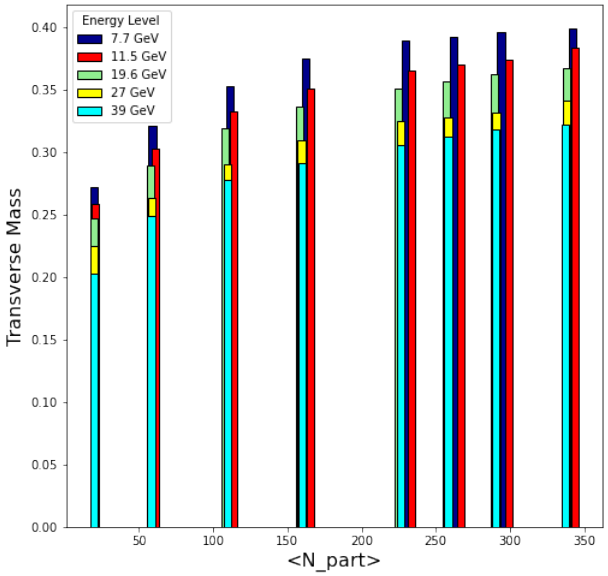

Figure 1: A bar chart for all energy levels of the transverse mass as a function of $\langle N_{part} \rangle$ from Au + Au collisions.

would be the line charts in Figure 5 and Figure 6. This is because we are interested in observing and comparing the

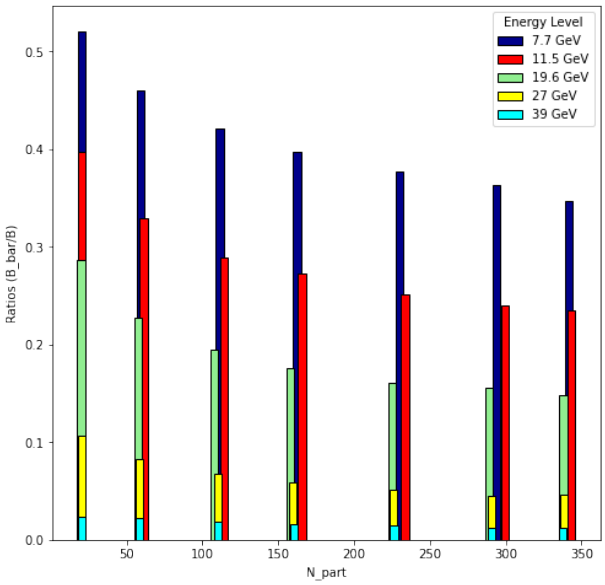

Figure 2: A bar chart for all energy levels of the antibaryon-to-baryon ratios as a function of $\langle N_{part} \rangle$ from Au + Au collisions.

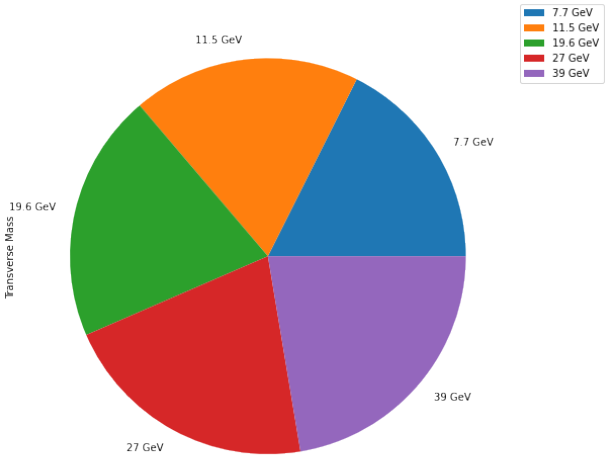

Figure 3: A pie chart for the total transverse masses of each energy level from Au + Au collisions.

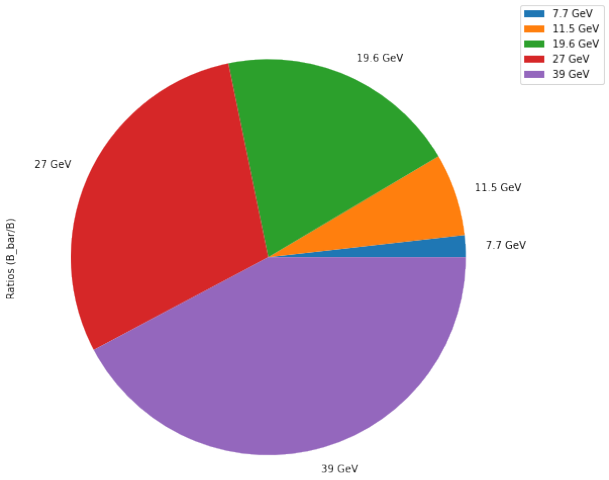

Figure 4: A pie chart for the antibaryon-to-baryon ratios of each energy level from Au + Au collisions.

trends of each energy level for the antibaryon-to-baryon ratios and transverse masses as functions of $\langle N_{part} \rangle$. This data would be similar to a time series used in line charts, but instead based on the average number of participating nucleons, $\langle N_{part} \rangle$. As such, a pie chart would be less suitable for these data sets since they do not account for the independent variable and only compares the total values of the antibaryon-to-baryon ratios and transverse masses for each energy level. Pie charts are also less suitable because they are used to display categorical data, whereas the data used here are quantitative measurements with independent and dependent variables. Similarly, bar charts are also used to display categorical data to compare the frequencies, relative frequencies, or percentages of various categories. Though this data has categories of energy levels, each independent dataset contains quantitative data whose trends as a function of $\langle N_{part} \rangle$ we want to compare to determine if they are significantly different.

3. Analysis

3.1. *Modelling and Fittin Data*

The first analysis we will present is the modelling and fitting of the antibaryon-to-baryon ratio and transverse mass data from Au+Au collisions as functions of $\langle N_{part} \rangle$. Using the line charts with error bars from Section 2, model fitting was used to create models of all energy levels from 7.7-39 GeV.

Figure 7 displays the model fitted antibaryon-to-baryon ratios as a function of $\langle N_{part} \rangle$. This plot uses a model-fitting polynomial function with a degree of four. The parameters of this plot are tabulated in Table 1, with A, B, C, D, and E corresponding to the coefficients of a polynomial model with a degree of fit equal to four:

$$Ax^4 + Bx^3 + Cx^2 + Dx + E. \quad (1)$$

Observing the five models of the antibaryon-to-baryon ratios versus $\langle N_{part} \rangle$ for each energy level in Figure 7, it can be seen that each data set increases as the energy level increases, with the 7.7 GeV model being at the bottom and the 39 GeV energy level at the top. The magnitude of the ratios is observed to get bigger for higher energy levels. The models also steadily flattens for lower energy levels with the higher energy levels having a slightly decreasing trend as $\langle N_{part} \rangle$ increases. These differences between the datasets could indicate that they are significantly different from one another, but further analysis is required to confirm the hypothesis. To determine which polynomial model fits our antibaryon-to-baryon data the best, we can compare their coefficient of determination values, R^2, and see which

Table 1: Antibaryon-to-baryon ratios versus $\langle N_{part} \rangle$ parameters with a degree of fit four for all energy levels.

Coefficient	7.7 GeV	11.5 GeV	19.6 GeV	27 GeV	39 GeV
A	-3.78×10^{-12}	2.42×10^{-11}	4.36×10^{-11}	5.91×10^{-11}	2.91×10^{-11}
B	2.82×10^{-9}	-2.03×10^{-8}	-4.14×10^{-8}	-5.28×10^{-8}	-3.11×10^{-8}
C	-5.86×10^{-7}	6.37×10^{-6}	1.45×10^{-5}	1.75×10^{-5}	1.21×10^{-5}
D	-1.37×10^{-5}	-0.001	-0.002	-0.003	-0.002
E	0.02	0.124	0.33	0.45	0.56
R^2	0.9960	0.9999	0.9981	0.9992	0.9993

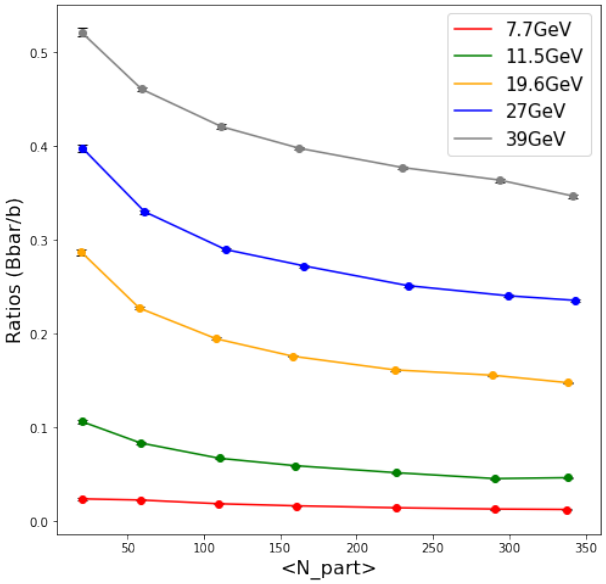

Figure 5: The antibaryon-to-baryon ratios as a function of $\langle N_{part} \rangle$ from Au + Au collisions in different energy levels.

yields the highest. From Table 1, it can be seen that the model for the 11.5 GeV energy level is the best fit for our data, with the highest R^2 value of 0.9999. As such, the model equation for our best fit would be:

$$(2.42 \times 10^{-11})x^4 + (-2.03 \times 10^{-8})x^3 + (6.37 \times 10^{-6})x^2 - 0.001x + 0.124. \quad (2)$$

The transverse mass models, similar to the antibaryon-to-baryon ratio models, increase in magnitude as the energy level increases. Unlike the antibaryon-to-baryon ratio models, though, all energy levels increase as $\langle N_{part} \rangle$ increases. The transverse mass model parameters for each energy level are tabulated in Table 2, including all coefficients and R^2 values. The best-fit model for this transverse mass versus $\langle N_{part} \rangle$ data would be the 19.6 GeV model since it has the highest R^2 value of 0.9999. Thus, the model equation would be:

$$(-3.06 \times 10^{-11})x^4 + (2.81 \times 10^{-8})x^3 + (-9.74 \times 10^{-6})x^2 - 1.71 \times 10^{-3}x + 2.17 \times 10^{-1}. \quad (3)$$

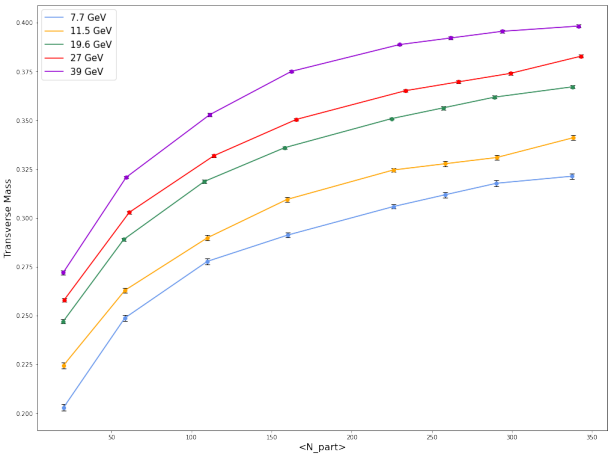

Figure 6: Transverse mass as a function of $\langle N_{part} \rangle$.

3.2. *Hypothesis Testing*

3.3. *Two Sample Independent t-Test*

To determine whether the data sets are significantly different for the antibaryon-to-baryon ratio data, we can use a two-sample unpaired t-test to compare the values between two independent groups, with the groups being two data sets of antibaryon-to-baryon ratio data. This type of test requires the variance of the difference between the means of the two groups, which can be done in Python using a scipy function. Since an unpaired t-test is parametric, the data is required to follow a normal distribution or approximately normal. As such, the data sets were checked to see if the $\frac{\bar{B}}{B}$ ratios from each different energy level are distributed normally. This was done using the scipy.stats normalcy test in Python, where a p-value was determined for each energy level and checked to see if each was greater than 0.05, thus yielding a normal distribution. Observing Table 3, it can be seen that all p-values for each energy level are above 0.05, making all data sets normally distributed. Thus, we can use the parametric unpaired t-test to test the hypothesis that data sets of different energy levels are significantly different.

The data we will be using are the energy levels of 19.6 GeV and 27 GeV. The null hypothesis for this hypothesis test is that the average values of antibaryon-to-baryon ratios from testing two different energy levels (19.6 GeV

Table 2: Transverse mass versus $\langle N_{part} \rangle$ parameters with a degree of fit four for all energy levels.

Coefficient	7.7 GeV	11.5 GeV	19.6 GeV	27 GeV	39 GeV
A	-4.95×10^{-11}	-6.78×10^{-12}	-3.06×10^{-11}	-1.89×10^{-11}	-2.36×10^{-11}
B	4.24×10^{-8}	1.04×10^{-8}	2.81×10^{-8}	2.03×10^{-8}	2.33×10^{-8}
C	-1.33×10^{-5}	-5.38×10^{-6}	-9.74×10^{-6}	-8.11×10^{-06}	-9.10×10^{-6}
D	2.03×10^{-3}	1.30×10^{-3}	1.71×10^{-3}	1.61×10^{-3}	1.79×10^{-3}
E	1.67×10^{-1}	2.01×10^{-1}	2.17×10^{-1}	2.29×10^{-1}	2.40×10^{-1}
R^2	0.9998	0.9987	0.9999	0.9993	0.9992

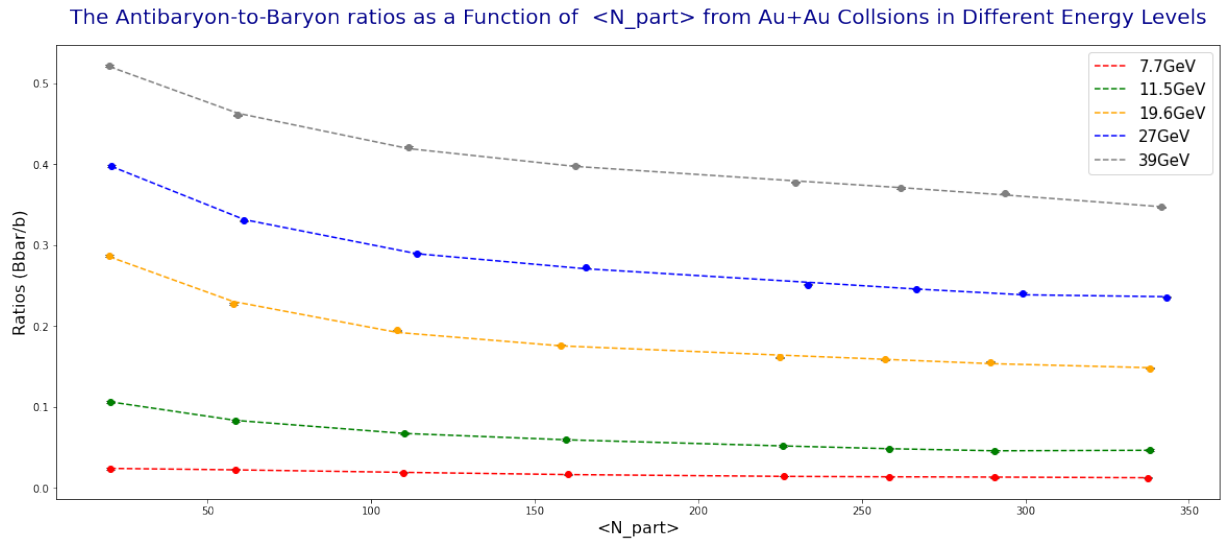

Figure 7: The antibaryon-to-baryon ratios as a function of $\langle N_{part} \rangle$ from Au + Au collisions in different energy levels.

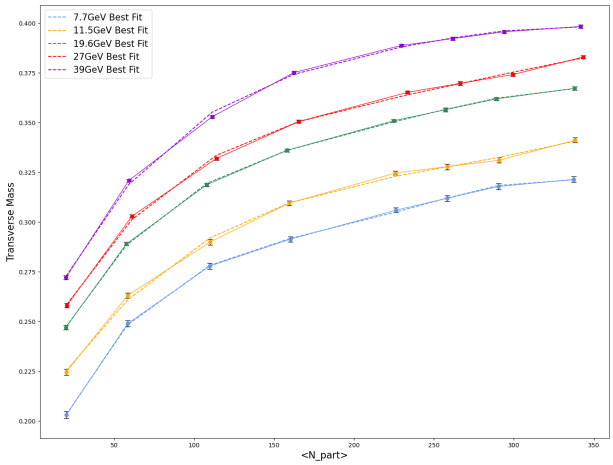

Figure 8: Transverse mass as a function of $\langle N_{part} \rangle$.

and 27 GeV) are the same. The alternative hypothesis would be that the average values of antibaryon-to-baryon ratios from testing two different energy levels (19.6 GeV and 27 GeV) are not the same. Using the antibaryon-to-baryon ratios of 19.6 GeV and 27 GeV, the p-value from the two-sample independent t-test gives a value of 0.003. Since the p-value is less than a significance level of 0.05,

Table 3: P-value for each $\frac{\bar{B}}{B}$ energy level using stats.normaltest function in Python.

Energy Level (GeV)	P-Value
7.7	0.46
11.5	0.14
19.6	0.06
27	0.08
39	0.22

we can reject the null hypothesis and claim that the data sets are significantly different.

3.4. *One-Way ANOVA*

To determine whether there are significant changes in the transverse mass within the centre-of-mass energy from 7.7-39 GeV, we can conduct a one-way ANOVA test. This type of test can compare the means of more than two groups by analyzing variances to infer the mean differences between the groups. ANOVA then uses the F-test to check the group's mean equality. Since the one-way ANOVA test is parametric, we must check to see if the transverse mass data is normally distributed. Similar to Section 3.3, this was

done using the scipy.stats normalcy test in Python by finding the p-value for each energy level and checking whether each was greater than 0.05, giving a normal distribution. Table 4 tabulates the p-values for each energy level. Since all p-values are greater than 0.05, all energy level data sets for the transverse mass are distributed normally. Thus, we can use the parametric one-way ANOVA to test the hypothesis.

Table 4: P-value for each transverse mass energy level using stats.normaltest function in Python.

Energy Level (GeV)	P-Value
7.7	0.13
11.5	0.26
19.6	.21
27	0.18
39	0.12

The null hypothesis for this hypothesis test is that there are no significant changes in the transverse mass within the centre-of-mass energy from 7.7-39 GeV. The alternative hypothesis would be that there is significant changes in the transverse mass within the centre-of-mass energy from 7.7-39 GeV. The one-way ANOVA testing performed with the transverse mass distribution at five different energy levels resulted in a F statistic of 4.32 and a p-value of 0.01. Since the p-value is less than the significance level of 0.05, we can reject the null hypothesis and conclude there are significant differences in the transverse mass within the five different centre-of-mass energies. Table 5 displays the additional detailed results of the one-way ANOVA test aside from the F statistic and p-value, including the degrees of freedom and sum and mean squared value for the energy and residual.

Table 5: ANOVA test results for the transverse mass distribution at five different energy levels.

	df	sum sq	mean sq
Energy	4.0	0.03	0.01
Residual	35.0	0.06	1.77×10^{-3}

4. Discussion

Our results can be compared to Adam et al. 2020 to observe any similarity in the relationships we found in our analysis to the ones found in the literature. Adam et al. 2020 found that the averaged transverse mass value of each particle species increases with the increasing $\langle N_{part} \rangle$ at all energy levels. The literature contains similar results to our analysis, as shown in Section 3.1 where the transverse mass as a function $\langle N_{part} \rangle$ models displays an increasing transverse mass as $\langle N_{part} \rangle$ increases for all models. Thus, our analysis confirms the result from Adam et al. 2020 that there is an increase in transverse mass as $\langle N_{part} \rangle$ increases, indicating the gradual development of collective motion with the increasing medium volume. Comparing the plots of the transverse mass as a function of $\langle N_{part} \rangle$ in Figure 13 of Adam et al. 2020 to our models in Figure 8, the observed relationship in both show an increasing transverse mass as $\langle N_{part} \rangle$ increases, with the slope gradually decreasing as $\langle N_{part} \rangle$ increases. The gradually decreasing slope in Figure 8 can confirm the literature result in Adam et al. 2020 that the transverse mass increases faster toward central collisions for hyperons for all energies. Both plots also have the trends being higher in transverse mass when the energy level increases, with 7.7 GeV being at the lowest and 39 GeV at the highest. This analysis confirms the result in Adam et al. 2020 that the transverse mass for the strange hadron Λ shows an increasing trend with the increasing collision energy.

Since the transverse mass is related to the centrality of the particle collisions, it is logical to assume that increasing the number of colliding particles will result in an increase in transverse mass. Because $\sqrt{s_{NN}}$ is the nucleon-nucleon centre-of-mass energy, an increase in this value will also relate to the centrality of the collision. Thus, at higher $\sqrt{s_{NN}}$, more transverse mass is collected. Combining these relationships, it could be true and logical to assume the result of the transverse mass versus $\langle N_{part} \rangle$ plot makes sense.

For the antibaryon-to-baryon ratio results, Adam et al. 2020 found that the ratios show significant decreases from the edge to the central collisions. This relationship between the antibaryon-to-baryon ratios in the literature can be confirmed with our models of the ratios as a function of $\langle N_{part} \rangle$ in Figure 7. In Figure 7, all energy models decline from the left side towards the centre, which is similar to the relationship found by Adam et al. 2020 in their Figure 20.

One aspect of antibaryon-to-baryon ratios is their sensitivity to the energy levels at which particle collisions occur. Theoretical models predict that the production of antibaryons and baryons is influenced by the energy available for particle interactions, as well as the temperature and density of the medium created in these collisions. As a result, variations in the energy of the collisions can lead to observable changes in the relative abundance of antibaryons compared to baryons. We have rejected the null hypothesis that states the average values of antibaryon-to-baryon ratios from testing two different energy levels (19.6 GeV and 27 GeV) are the same. Our results provide additional support for the idea that the relative abundance of antibaryons and baryons is influenced by collision energy, indicating complex interactions between particle production mechanisms and the properties of the medium.

References

Adam, J., Adamczyk, L., Adams, J. R., Adkins, J. K., Agakishiev, G., Aggarwal, M. M., Ahammed, Z., Alekseev, I., Anderson, D. M., Aoyama, R., et al. (Sept. 2020). "Strange hadron production in Au + Au collisions at $\sqrt{s_{NN}}$ = 7.7, 11.5, 19.6, 27, and 39 GeV". In: *Phys. Rev. C* 102 (3), p. 034909. DOI: 10.1103/PhysRevC.102.034909. URL: https://link.aps.org/doi/10.1103/PhysRevC.102.034909.